

Measuring Turbulent Dissipation Rates Beneath an Antarctic Ice Shelf

AUTHORS

Emily Venables

Keith Nicholls

British Antarctic Survey,
Natural Environment Research
Council, Cambridge, UK

Fabian Wolk

Rockland Scientific, Inc.,
Victoria, BC

Keith Makinson

Paul Anker

British Antarctic Survey,
Natural Environment Research
Council, Cambridge, UK

Introduction

Ice shelves are the floating extension of a grounded ice sheet. As an ice sheet flows toward the coast, it thins to the point where it finally goes afloat. Where it goes afloat is called the grounding line. The ice then carries on flowing out to sea, the seaward edge being the calving front, or ice front. This is where icebergs calve episodically. Ice shelves gain ice from the ice flowing from the ground-based ice sheet and from snowfall, and they lose ice by basal melting and by icebergs calving.

Ice shelves have global significance. The presence of an ice shelf can affect the rate at which inland ice flows into the ocean. If the restraint imposed by an ice shelf is reduced, inland ice flows into the ocean more rapidly, with a direct effect on global sea level (Schoof, 2007). Furthermore, Antarctic ice shelves cover around 40% of the area of the continental shelf and play

ABSTRACT

Microstructure shear, temperature, and conductivity observations from a tethered profiler have been made beneath George VI Ice Shelf to examine processes driving vertical heat flux in the oceanic turbulent boundary layer. Such measurements at the ice-ocean interface within the cavity of an ice shelf are unprecedented, requiring the deployment of a profiler through 400-m deep access boreholes. We describe the drilling technique developed for this purpose, which involves using a brush to widen the deepest section of the borehole, and as evidence that this novel technique can be successful, we present shear and thermal variance spectra from the profiler. These spectra indicate that dissipation rates of turbulent kinetic energy, from which heat flux can be calculated, can be resolved beneath an ice shelf as well as they can be in open water.

Keywords: turbulence, microstructure, basal melting, hot-water drilling

a major role in water mass transformations that have global influence through deep water formation and overturning circulation.

In a changing climate, the rate at which ice shelves melt into the ocean is likely to change, and to be able to predict that change, we need to understand the controls on the rate of basal melting. Essentially, that entails learning the controls on the rate at which heat and salt can be transported vertically through the boundary layer at the ice shelf base. The ability to measure turbulent dissipation rates in the boundary layer would therefore be a powerful tool in helping characterize the mixing regime.

Here we present turbulence microstructure data collected from the boundary layer beneath an Antarctic ice shelf, using a free-falling Rockland Scientific Inc. (RSI) VMP200 profiler. The results demonstrate that this type of instrument is capable of gathering scalar and velocity microstructure data from this unique but difficult-to-

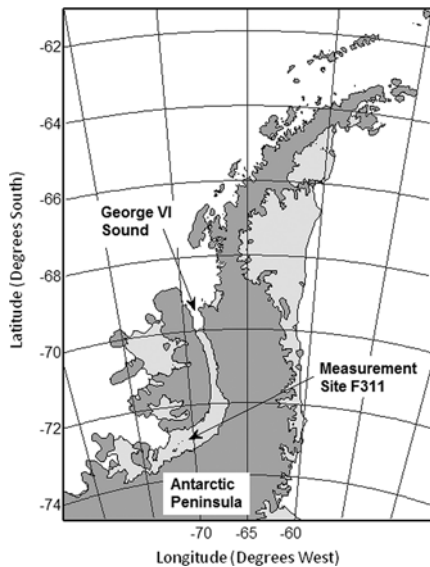
access environment. We first describe the measurement site and the suite of instrumentation that was used. We then discuss details of the VMP200 itself and the way in which it was deployed in this novel environment. Finally, we show examples of the data that were obtained.

The Measurement Site

George VI Ice Shelf, Antarctica, is the largest ice shelf on the west coast of the Antarctic Peninsula (Figure 1). It occupies George VI Sound, lying between Alexander Island and the mainland. The ice shelf is fed principally by a combination of ice flow from glaciers on the mainland to the east (Bishop & Walton, 1981) and from in situ snowfall. At its southern ice front, the ice is around 150 m thick. To the east, the ice thickness increases rapidly to a maximum of around 450 m, before gradually decreasing toward a value of around 100 m at the northern ice front (Lythe

FIGURE 1

Map showing the location of the field site on George VI Ice Shelf. Light gray areas mark ice shelves and dark gray areas mark land.



& Vaughan, 2001). The ice shelf is a narrow feature, around 440 km in length and varying from 23 to 60 km in width; it is underlain by a water column up to 800 m thick (Maslanyj, 1987).

The site selected for the present study (S 72°49.9', W 070°50.6') was on the basal slope to the west of the thickest part of the ice shelf, some 50 km from the southern ice front. At this site, the ice was 381 m thick, overlying a 636-m-thick water column. It was occupied by a team of six from December 27, 2011 until January 19, 2012. During that time, a hot water drill was used to create two access holes through the ice shelf for the installation of instruments for long-term measurements, primarily in the boundary layer. Prior to the installation, a Seabird Fast-Cat (SBE49) conductivity-temperature-depth (CTD) profiler was used to obtain a sequence of CTD profiles and an RSI VMP200 was used to obtain microstructure turbulence profiles through the boundary layer.

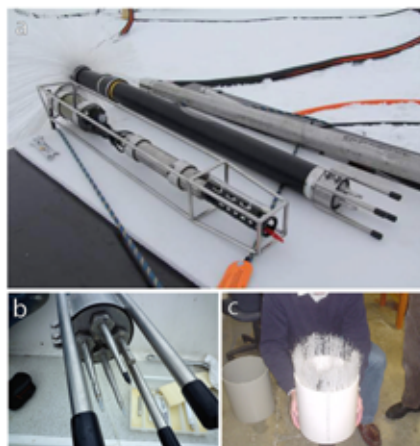
The VMP200

The VMP200 (Figure 2) is a standard vertical turbulence microstructure profiler (Wolk et al., 2002) equipped with two standard velocity shear probes (Osborn & Crawford, 1980), a fast-response thermistor (FP07) and a microconductivity sensor (Seabird SBE7), yielding derived turbulence parameters $\partial u/\partial z$, $\partial v/\partial z$, $\partial T/\partial z$, and $\partial C/\partial z$, respectively. In addition, the profiler carries depth, vibration, and tilt sensors. The turbulence sensors are mounted on the forward nose bulkhead (Figure 2b) so that they are in the undisturbed flow.

The profiler has a total length of 1.5 m, and the diameter of the main pressure housing is 0.12 m. The diameter of the brush is approximately 0.9 m when the brush is in its natural position. The brush filaments are made from nylon and flex easily during profiling through the water column

FIGURE 2

(a) VMP200 profiler (center) showing the forward sensor array in the foreground and the drag brushes in the background. (b) Detail of the turbulence sensors: two shear probes (white tips) and an FP07 fast thermistor (black tip). SBE7 microconductivity sensor is not shown. (c) Demonstration of how the rear drag brush flexes during profiling through the water or ice hole.



or the borehole (Figure 2c). This feature was essential for the deployment through the ice hole, as will be described in the following section.

All turbulence channels are sampled at a rate of 512 Hz, and ancillary sensors, such as pressure and tilt, are sampled at 64 Hz. Signals from high-frequency sensors (shear probes, thermistor, microconductivity probe, and vibration sensors) and the pressure sensor are differentiated electronically before recording to improve signal resolution (Mudge & Lueck, 1994). Before sampling, an anti-aliasing filter is applied at 98 Hz to prevent vibration noise signals or other spurious high-frequency data entering the signal band of the turbulence fluctuations. All readings are transmitted through an electro-mechanical cable to a data acquisition computer at the surface of the ice shelf. The real-time transmitting option of the profiler was selected over internal recording in order to ensure successful data recovery in case the profiler should get irretrievably stuck in or underneath the ice shelf.

The profiler uses a tail brush to provide drag to control its descent rate and to provide a stabilizing torque to ensure the profiler moves in a direction parallel to its principal axis (analogous to the flight of a dart). This ensures that the angle of attack for the shear sensors is within their tolerance (typically within 15° of the profiler's principal axis). The optimal descent rate (in this case 0.7–0.9 m s⁻¹) is a compromise between the requirement to profile fast enough to satisfy the Taylor “frozen fluid” hypothesis that the measured parameter does not change in space over the time in which the sensor passes through it and slow enough to maximize the vertical resolution of the scalar sensors. An additional consideration is that higher profiling speeds

result in higher levels of profiler vibration. Although this range is optimal, slightly slower speeds can still yield good turbulence data, particularly those derived from the temperature gradient.

Deploying the Instrument Beneath the Ice Shelf

Vertical microstructure profilers determine the dissipation rate directly by measuring velocity shear at the dissipation scale, and they are an established tool for use in the open ocean. Obtaining good shear measurements requires the profiler to descend smoothly and freely in order to minimize vibration contamination of the measured shear signals. In the case of tethered profilers such as the VMP200, it is important for the tether not to affect the free descent of the profiler or to impart cable vibration or ship motion. The tethered operation of the profiler therefore requires excess cable to be deployed to ensure that the instrument is falling as freely as possible.

Deployment of tethered profilers beneath ice shelves presents two principal difficulties. First, the standard style of brush would require a large diameter borehole that would demand an unfeasibly large amount of fuel. Second, the tether may not pass down the borehole in a way that does not create vibrations that would contaminate the shear sensor data.

A pressurized hot water drill (Makinson & Anker, 2014) was used to create an access hole through the 381-m ice shelf. The drill supplies 90 L min⁻¹ of 80°C water to the nozzle, equivalent to a thermal power of a little over half a megawatt. Drilling at a speed of around 0.9 m min⁻¹ provided an access hole at least 0.3 m in diameter. The lowest ambient temperature in the ice shelf was about -12°C,

which results in an initial refreezing rate of approximately 0.5 cm of diameter per hour, falling to 0.25 cm per hour after approximately 1 h.

The nozzle is a forward-pointing, full cone jet of half-angle 7.5° while drilling the porous firn and is then changed to a 0° forward jet once solid ice is reached. The nozzle is mounted on a heavy pipe (>50 kg) to provide the weight necessary to keep the hole vertical and counteract the forward momentum of the water. During drilling, the nozzle is lowered slowly enough to make a hole with a diameter sufficient to allow the nozzle to pass through, with much of the widening of the hole taking place over several meters above the nozzle (Figure 3a). When the nozzle finally penetrates the base of the ice shelf, the hot water from the forward-pointing jet is lost to the ocean, and the widening of the hole above the nozzle ceases once any residual heat has been used. The result is a narrowing or “necking” in the hole at the ice base (Figure 3b). Although the majority of the hole has a diameter of 30 cm, allowing the unrestricted passage of the profiler, the necking would prevent the brush from passing through the final few meters.

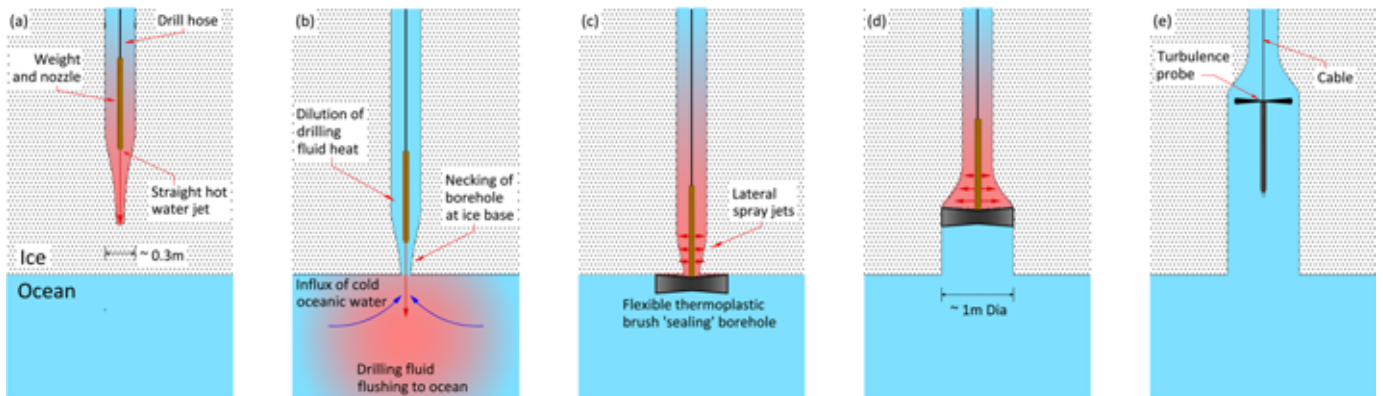
An additional but related difficulty came from the need to have the microstructure profiler working effectively as soon as possible after leaving the borehole, as the aim of the experiment was to investigate the dynamics within the boundary layer. Once free of the hole, we require that the profiler rapidly attains terminal velocity and smooth motion. To minimize the time taken to attain smooth descent, a novel technique was used to enlarge the borehole over the last few meters, thus removing the necking effect and creating a “VMP garage” for parking the instrument just above the ice shelf base.

Once the drill nozzle was recovered, the forward-pointing jet was replaced with a 1-m diameter drill brush and eight sideways-pointing fan sprays installed in a segment immediately above it. The bristles of the brush were 1 mm in diameter, and the whole brush assembly flexible enough to be pushed down the 30-cm diameter borehole by the weight of the nozzle. The fan sprays had a vertical angular coverage of ±10° and a horizontal spray angle of 95°. The reconfigured nozzle was then lowered down the borehole and dropped through the ice shelf base (Figure 3c). The progress of the brush was monitored by noting the change in tension on the drill hose. The nozzle was then raised until the hose tension started to increase, indicating that the brush was being pulled into contact with the base of the ice. At this point, the winch was stopped and water was allowed to continue to flow into the bottom of the borehole, the brush largely preventing the loss of heat to the sea. The nozzle was then slowly raised for a few meters to enlarge the hole at the base to create the garage.

Two methods of lowering the VMP200 through the boundary layer from its garage were attempted to see whether the instrument could be made to descend smoothly enough to give uncontaminated shear profiles. The first was to maintain slack cable at the top of the borehole and allow the cable to run into the hole largely unchecked. The second method was to run the cable from the winch, with the winch paying out at close to full speed. An examination of the spectra from the shear sensors suggests that there is little to choose between the two techniques. The second approach was the most convenient and was adopted as the standard method. Once released from its garage, profiles

FIGURE 3

Diagrams of the borehole at each stage of the drilling and profiling process. (a) Drilling process demonstrating melt profile. (b) Breakthrough of ice base to ocean, bypassing of drilling fluid and necking of borehole. (c) Use of brush and fan sprays isolating drilling fluid from ocean. (d) Upward progression of brush and fan sprays opening up borehole. (e) Widened borehole enabling unrestricted deployment of microstructure profiler.



of fall speed show that the VMP was falling at 0.4 m s^{-1} as it crossed the depth of the ice base and continued to accelerate to its profiling speed of 0.8 m s^{-1} within a distance of 5 m of the ice base. During the period of acceleration beneath the ice base, inclinometer data show that the profiler was falling vertically (within 1°). We are therefore confident that the data from immediately beneath the ice base are useable.

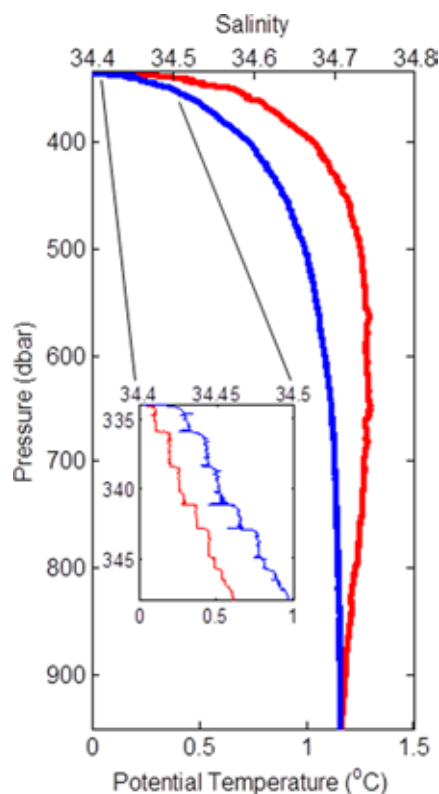
As the diameter of the borehole was gradually reducing by refreezing, relatively few profiles could be obtained before the hole needed to be re-widened with the hot water drill, a process constrained by the limited supply of fuels. In total, 19 microstructure profiles were obtained, and in addition to the VMP200 casts, standard CTD profiling was carried out to monitor the evolution of the water column.

Results

The CTD profiler was used to obtain an initial view of the oceanographic conditions beneath the ice shelf (Figure 4). Well below the ice-shelf base, the water properties were

FIGURE 4

Example CTD temperature (red) and salinity (blue) profile, with inset showing detail of staircase. (Color versions of figures available online at: <http://www.ingentaconnect.com/content/mts/mts/2014/00000048/00000005>.)

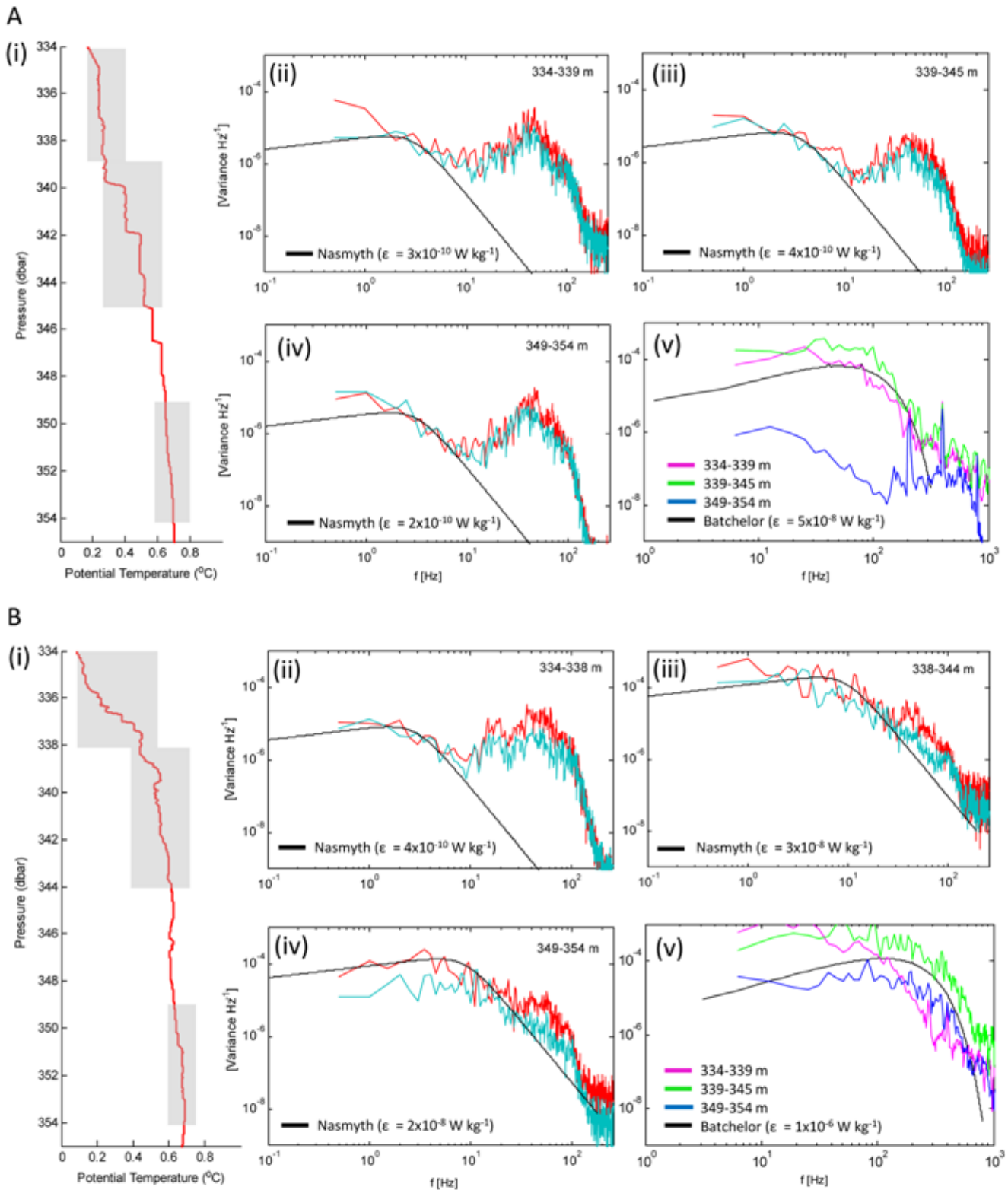


consistent with the ambient conditions observed in the past over the open continental shelf to the west (Figure 1); these consist of relatively warm Circumpolar Deep Water that intrudes onto the continental shelf in this sector of the Antarctic (e.g. Jenkins & Jacobs, 2008). All ice shelves in contact with this water have high basal melt rates, and it is important that the way in which the heat is transferred through mixing to the ice base is understood. Within 50 m of the ice base, the effect of the ice shelf is clearly evident from the cooling and freshening of the water column. This configuration of cold fresh water overlying relatively warm and salty water raises the possibility of double diffusive convection (Turner, 1973). Although many access holes have been made through ice shelves, this is the first time the effects of diffusive convection have been apparent, with a well-defined thermohaline staircase visible in both the temperature and the salinity profiles (Figure 4, inset).

The VMP was used to investigate the boundary layer in greater detail. The thickness of the well-mixed layers typically ranges between 1 and

FIGURE 5

VMP data from a strongly staircased environment (A) and a mixed environment (B) in the same location beneath George VI Ice Shelf. In each case, we show (i) a temperature profile, (ii–iv) shear spectra from the two channels (red and blue) with a theoretical Nasmith spectrum scaled for the shown dissipation rate, and (v) temperature gradient spectra from the same depth segments with a theoretical Batchelor spectrum scaled for the shown dissipation rate. The gray areas on the profiles correspond to the depth segments used for each set of spectra.



6 m, and the temperature step between layers is between 0.1°C and 0.2°C. Figure 5 shows two temperature profiles from the same site and the shear and thermal variance spectra for various depth ranges. Dissipation spectra were calculated using two independent methods, one using velocity shear variance and the other thermal variance. We followed the processing technique of Sirevaag and Fer (2012), using the method of Ruddick et al. (2000) to fit the Batchelor spectrum to observed temperature gradient spectra. Each shear spectrum was calculated using a 1-s, half-overlapping window within the relevant depth range. A 3-s window was used for the thermal variance spectra to allow more averaging.

The quality of shear data was assessed according to how well the spectral shape of the shear variance agreed with the Nasmyth empirically derived universal spectrum for oceanic turbulence (Oakey, 1982). Vibration noise is evident in the spectra of shear probes and the vibration sensor (not shown) at around 50 Hz. This is outside the range of interest for dissipation measurements as it is above the Kolmogorov frequency cut-off of approximately 10 Hz for the computed dissipation rate values of $\sim 10^{-10} \text{ W kg}^{-1}$. In addition, shear spectra steeply rise below ~ 1 Hz as a result of low-frequency profiler motion. This motion is particularly strong in the beginning of the profile just under the ice-base, where the VMP exits from the garage and accelerates. The measured profiler tilt is around $\pm 0.5^\circ$ in the first few meters of the cast before settling down to $\pm 0.25^\circ$. Careful examination of spectra from 1-m segments of the profile suggests that the noise level for this operating environment is $\epsilon \sim 10^{-10} \text{ W kg}^{-1}$.

Figures 5A-i and 5B-i show temperature profiles from the same loca-

tion, 6 h apart. The “staircase” is much less well established in Figure 5B, and there are numerous inversions of temperature that may be salinity compensated indicating a better-mixed environment. Shear variance spectra conformed relatively well to the universal shape of Nasmyth in this environment (Figures 5Biii and 5Biv), although there is still evidence of vibration contamination at around 50 Hz, which elevates the spectra above the Nasmyth curve. In stably stratified regions, particularly where thermohaline steps were less than 2 m in height, the shear spectra are poor (e.g., Figures 5Aii–5Aiv).

Thermal gradient spectra were generally much better resolved than the velocity shear spectra within the staircase; they were poorly resolved only in well-mixed regions where there was very little thermal structure such as the deepest section of Profile A (Figure 5A-v). Generally, the scaled thermal gradient spectra yielded a dissipation rate two orders of magnitude greater than the shear spectra, but this can most likely be attributed to the environment rather than the deployment technique. Further scientific analysis of these results and the oceanographic environment beneath George VI Ice Shelf will be addressed in future publications.

Summary and Conclusions

When operating from research vessels, great care is taken to ensure that a tethered microstructure profiler is truly free-falling and to minimize vibrations from the tether. This is more of a challenge when operating beneath an ice shelf, where the tether has to run through several hundred meters of borehole before emerging into open water beneath the ice. We have

shown, however, that it is possible to operate a free-fall microstructure profiler beneath an ice shelf and obtain shear and temperature microstructure profiles through a 381-m borehole that is 0.3 m wide. In this case, the water was relatively quiescent, and the procedure is yet to be tested in an area with strong currents.

Microstructure profiles were collected from the boundary layer beneath George VI Ice Shelf, Antarctica, using a standard VMP200 instrument. A more detailed discussion of the physical environment, along with careful estimates of dissipation rates derived from both shear variance and thermal variance, will be given in subsequent publications. So far, the study demonstrates the feasibility of a technique that will yield an improved understanding of the way heat and salt are transferred from the ocean, through a stratified boundary layer, to the base of ice shelves. This should lead to better parameterizations of vertical mixing that will improve our ability to predict changes in Antarctic ice shelves.

Acknowledgments

This work was funded by the Natural Environment Research Council grant NE/H009205/1. The authors would like to thank Rolf Lueck for providing helpful comments during the preparation of this manuscript and Laurie Padman and two anonymous reviewers for their reviews, which improved it even further.

Corresponding Author:

Emily Venables
British Antarctic Survey,
Natural Environment Research
Council, Cambridge, UK
Email: eminab@nerc.ac.uk

References

- Bishop**, J.F., & Walton, J.L.W. 1981. Bottom melting under George VI Ice Shelf, Antarctica. *J Glaciol.* 27(97):429-47.
- Jenkins**, A., & Jacobs, S. 2008. Circulation and melting beneath George VI Ice Shelf, Antarctica. *J Geophys Res.* 113:C04013. <http://dx.doi.org/10.1029/2007JC004449>.
- Lythe**, M.B., & Vaughan, D.G. 2001. BEDMAP: A new ice thickness and subglacial topographic model of Antarctica. *J Geophys Res.* 106(B6):11335-51. <http://dx.doi.org/10.1029/2000JB900449>.
- Makinson**, K., & Anker, P.G.D. 2014. The BAS ice shelf hot water drill: design, methods and tools. *Ann Glaciol.* 55(68), in press.
- Maslanyj**, M.P. 1987. Seismic bedrock depth measurements and the origin of George VI Sound, Antarctic Peninsula. *Brit Antarc Surv B.* 75:51-65.
- Mudge**, T., & Lueck, R.G. 1994. Digital signal processing to enhance oceanographic observations. *J Atmos Oceanogr Tech.* 11:825-36. [http://dx.doi.org/10.1175/1520-0426\(1994\)011<0825:DSPTEO>2.0.CO;2](http://dx.doi.org/10.1175/1520-0426(1994)011<0825:DSPTEO>2.0.CO;2).
- Oakey**, N.S. 1982. Determination of the rate of dissipation of turbulent energy from simultaneous temperature and velocity shear microstructure measurements. *J Phys Oceanogr.* 12(3):256-71. [http://dx.doi.org/10.1175/1520-0485\(1982\)012<0256:DOTROD>2.0.CO;2](http://dx.doi.org/10.1175/1520-0485(1982)012<0256:DOTROD>2.0.CO;2).
- Osborn**, T.R., & Crawford, W.R. 1980. An airfoil probe for measuring turbulent velocity fluctuations in water. In: *Air-Sea Interaction: Instruments and Methods*, F.W. Dobson, & R. Davis, Eds., Plenum. 369-86.
- Ruddick**, B., Anis, A., & Thompson, K. 2000. Maximum likelihood spectral fitting: The Batchelor spectrum. *J Atmos Oceanic Technol.* 17:1541-55. [http://dx.doi.org/10.1175/1520-0426\(2000\)017<1541:MLSFTB>2.0.CO;2](http://dx.doi.org/10.1175/1520-0426(2000)017<1541:MLSFTB>2.0.CO;2).
- Schoof**, C. 2007. Ice sheet grounding line dynamics: Steady states, stability, and hysteresis. *J Geophys Res.* 112:F03S28. <http://dx.doi.org/10.1029/2006JF000664>.
- Sirevaag**, A., & Fer, I. 2012. Vertical heat transfer in the Arctic Ocean: The role of double-diffusive mixing. *J Geophys Res Oceans.* 117(C7): C07010. <http://dx.doi.org/10.1029/2012JC007910>.
- Turner**, J.S. 1973. *Buoyancy Effects in Fluids*. Cambridge, UK: Cambridge University Press. 367 pp. <http://dx.doi.org/10.1017/CBO9780511608827>.
- Wolk**, F., Yamazaki, H., Seuront, L., & Lueck, R.G. 2002. A new free-fall profiler for measuring biophysical microstructure. *J Atmos Oceanogr Tech.* 19:790-3. [http://dx.doi.org/10.1175/1520-0426\(2002\)019<0780:ANFFPF>2.0.CO;2](http://dx.doi.org/10.1175/1520-0426(2002)019<0780:ANFFPF>2.0.CO;2).